Fall Detection Based on the Instantaneous Doppler Frequency: A Machine Learning Approach

Ali Chelli and Matthias Pätzold
Faculty of Engineering and Science, University of Agder, 4898 Grimstad, Norway.
Emails: {ali.chelli, matthias.paetzold}@uia.no

***Abstract*—Modern societies are facing an ageing problem which comes with increased cost of healthcare. A major share of this ever-increasing cost is due to fall related injuries, which urges the development of fall detection systems. In this context, this paper paves the way for building of a radio-frequency-based fall detection system. This paper presents an activity simulator that generates the complex channel gain of indoor channels in the presence of one person performing three different activities, namely, slow fall, fast fall, and walking. We built a machine learning framework for activity recognition based on the complex channel gain. We assess the recognition accuracy of three different classification algorithms: decision tree, artificial neural network (ANN), and cubic support vector machine (SVM). Our analysis reveals that the decision tree, ANN, and cubic SVM achieve an overall recognition accuracy of 73%, 84.1%, and 92.6%, respectively.**

I. Introduction

Advances in the diagnosis and treatment of diseases have led to an increase in the average age of the population and a surging number of older persons. Statistics show that the total number of people aged 65 and above reached 650 million in 2015 [1], and by 2050, this number will exceed two billion [2]. The society ageing problem leads to higher healthcare costs. For older people, the costs of non-fatal fall injuries reached USD 50 billion in 2015 [3], while falls were the leading cause of death in 2013 [4]. All these facts urge the development of fall detection systems to reduce the death toll of falls, decrease healthcare cost, and assist adults with an independent living difficulty.

In recent years, a plethora of fall detection systems have been developed using different approaches. Existing fall detection systems can be classified into three main classes: (i) context-aware systems, (ii) wearable device-based systems, and (iii) radio-frequency (RF)-based systems [5].

Context-aware systems leverage sensors deployed in specific monitoring areas. The monitoring sensors include mainly cameras, microphones, and pressure sensors. Camera-based fall detection systems apply classification algorithms to recorded video to detect falls [6]. The main limitations of camera-based context-aware systems are that they can violate users' privacy, cause a high deployment cost, and have a very limited monitoring area.

Wearable fall detection systems employ a device equipped with an accelerometer to detect changes in the acceleration. These changes are due to the user activity and can be analyzed to determine if a fall event has occurred. The use of wearable devices for activity recognition and fall detection has been extensively investigated in the literature [7], [8]. Wearable device-based systems have numerous advantages: (i) they can detect falls without violating user privacy, (ii) they have a low cost, and (iii) they have an unlimited monitoring area. However, if the user forgets to wear the device, fall detection becomes impossible, which is the major disadvantage of wearable device-based systems.

The third kind of fall detection systems is based on RF techniques. They do not require wearable devices and have limited privacy issues. The main idea behind RF-based fall detection systems is to extract the fingerprints of human activity from the received RF signal of a wireless system to detect falls. In [9], the authors use the channel state information obtained from a WiFi network card to detect falls. A three-dimensional (3D) motion tracking system that uses wireless signals to detect falls of a single person is developed in [10]. Several research works take the advantage of the widespread deployment of WiFi systems to develop solutions for human motion detection, gesture recognition, and indoor localization, while few focus on fall detection. The variations in the received signal strength of WiFi are utilized in [11] for gesture recognition. The authors of [12] propose an approach for human tracking based on wireless signals, but this approach cannot be used for human activity recognition.

As opposed to [9], where the channel state information is used to detect falls, we propose a new method for fall detection based on the instantaneous Doppler frequency. The main contributions of our paper are as follows:

- We develop an activity simulator that generates the complex channel gain of indoor channels in the presence of one person performing three dif-

This work was supported by the WiCare Project funded by the Research Council of Norway under grant number 261895/F20.

ferent activities: slow fall, fast fall, and walking.

- We propose a novel method for extracting the instantaneous Doppler frequency with high accuracy from the complex channel gain.
- We build a machine learning framework for activity recognition based on the complex channel gain and the instantaneous Doppler frequency.
- We assess the recognition accuracy of three different classification algorithms: decision tree, artificial neural network (ANN), and cubic support vector machine (SVM).
- We demonstrate that the decision tree, ANN, and cubic SVM achieve an overall accuracy of 73%, 84.1%, and 92.6%, respectively. These results are achieved by extracting just four features from the instantaneous Doppler frequency, which makes the proposed solution accurate, while its computational cost is low.

The remainder of the paper is organized as follows. Section II provides an overview of the proposed activity simulator, while the expression of the complex channel gain is derived in Section III. In Section IV, we discuss the pre-processing methods used to estimate the instantaneous Doppler frequency. Section V describes the machine learning framework and how we use it to recognize different types of activities. In Section VI, we assess the performance of the proposed framework and discuss the obtained results. Finally, Section VII offers concluding remarks.

II. Activity Simulator Overview

Our objective is to recognize human activities using machine learning applied to the complex channel gain of the radio propagation channel. To test this approach, we generate synthetic data emulating the complex channel gain of an indoor 3D environment in the presence of a single moving person as illustrated in Fig. 1. In this section, we provide a high-level overview of the channel simulator and describe how the data was generated for different activities. We consider 30 different participants with different heights performing three activities. The simulated activities include fast fall, slow fall, and walking. Each participant performs these activities inside a room with a size of 5 by 10 m. During the simulation, only one person is inside the room.

As the person moves inside the room, their coordinates change with time and a Doppler effect is generated by this movement. Our objective is to recognize the person's activity by analyzing the variation of the complex channel gain and the instantaneous Doppler frequency. This latter reflects how the Doppler frequency varies with time. To measure the complex channel gain, the room is equipped with fixed transmitter and receiver denoted by T_x and R_x, respectively. The T_x and R_x operate in the 2.4 GHz WiFi band. The transmitter T_x emits electromagnetic waves that propagate in the indoor environment. These waves are reflected by the objects located in the room before arriving at the receiver R_x. All the objects in the room are static apart from the moving person. Thus, the received signal contains the fingerprints of the user activity. Our objective is to use signal processing techniques together with machine learning to determine human activity based on the signal measured at the receiver R_x.

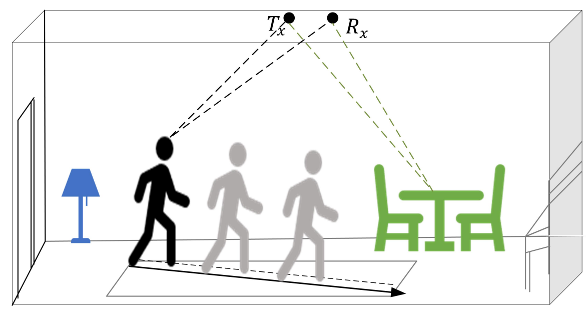

Fig. 1: A typical 3D indoor propagation scenario with one moving person.

For each participant, the complex channel gain is recorded for 120 s and then divided into 30 buffers of length 4 s. Each data buffer is labeled with the corresponding actual activity. For a given activity, the path followed by the participant is composed of 10 straight lines. The start and end points of each line are randomly generated. Hence, different participants follow different paths which makes the collected data more generic and more realistic. The height of each participant is randomly generated and evenly distributed in the interval [1.5 m, 1.9 m].

For the walking activity, the subject moves with a constant speed along a straight line. The value of the speed is the outcome of a random generator and is uniformly distributed in the interval [0.8 m/s, 1.2 m/s] [13]. For the falling activity, the participant first walks and then the fall starts. The duration of the fast fall and the slow fall are equal to 1 s and 2 s [14], respectively. When the fall starts, the participant's speed increases and reaches its maximum value right before the person hits the ground. The maximum speeds for the fast fall and the slow fall are equal to 2.6 m/s and 1.8 m/s, respectively [15]. After the fall, the person remains on the ground and their speed becomes equal to zero.

Using the described mobility model, we can compute the time-variant coordinates of the persons as they move inside the room. Knowing the locations of the transmitter T_x and the receiver R_x, we can determine the Doppler frequency associated with the human movement and subsequently compute the complex channel gain measured at the receiver R_x.

III. Complex Channel Gain

To measure the complex channel gain, the room is equipped with a transmitter T_x and a receiver R_x having as coordinates (x^T, y^T, z^T) and (x^R, y^R, z^R), respectively. The transmitter T_x emits electromagnetic waves that propagates in the indoor environment. These waves are reflected by the objects located in the room before arriving at the receiver R_x. During the data collection, only one person is moving and performing their activities in the room, while all the objects in the room are static. We model this moving person by a single moving scatterer S^M corresponding to the head. The initial position of S^M in the $x-y$ plane is given by (x^M, y^M) at time $t = 0$.

For the walking activity, the person moves with a constant speed along a path composed of 10 straight lines. For a given line in this path, the direction of motion α_v and the speed of motion v_h in the horizontal plane are constants. When the person walks along a new line, their direction of motion α_v is updated to a new value, while their speed v_h in the horizontal $x-y$ plane remains the same.

During walking, the time-variant positions $x(t)$ and $y(t)$ along the x- and y-axis of the moving scatterer S^M can be expressed as

$$x(t) = x^M + v_h \cos(\alpha_v)\, t \tag{1}$$

$$y(t) = y^M + v_h \sin(\alpha_v)\, t. \tag{2}$$

The time-variant position $z(t)$ of the scatterer S^M (the head) along the z-axis can be written as [16]

$$z(t) = h_{\text{step}} \cos(2\pi f_{\text{step}} t) + h_{\text{head}} \tag{3}$$

where h_{step}, h_{head}, and f_{step} refer to the step height of the head during walking, the person height, and the walking frequency, respectively. The walking frequency can be determined as $f_{\text{step}} = v_h/L_s$, where L_s is the stride length [13]. The value of the stride length is proportional to the person height. The vertical speed $v_v(t)$ along the z-axis can be computed by deriving $z(t)$ with respect to t, i.e., $v_v(t) = dz(t)/dt$. It is worth to mention that the validity of the head trajectory model in (3) has been confirmed by fitting it to real-world data obtained from tracking the head trajectory obtained from video recording [16].

We model the static objects in the room, such as the walls and the furniture, by N fixed scatterers S_n^F ($n = 1, 2, \ldots, N$). Thus, the complex channel gain can be expressed as a sum of two terms: (i) the first term captures the contribution of the moving scatterer S^M and (ii) the second term are the multipath components stemming from the N fixed scatterers S_n^F, i.e., [17]

$$\mu(t) = c_m \exp[j\theta_m(t)] + \sum_{n=1}^{N} c_n \exp(j\theta_n) \tag{4}$$

where the symbols c_m and c_n stand for the path gains associated with the moving scatterer and nth fixed scatterer, respectively. The phases θ_n are independent identically distributed random variables with uniform distribution in the interval $[0, 2\pi)$. The phase $\theta_m(t)$ associated with the moving scatterer is time-variant and can be determined as $\theta_m(t) = 2\pi \int_{-\infty}^{t} f_m(u)du$ [17], where $f_m(t)$ denotes the instantaneous Doppler frequency. This quantity can be computed as [18]

$$\begin{aligned} f_m(t) = -f_{\max}(t) \Big\{ &\cos(\beta_v(t)) \Big[\cos\left(\beta^T(t)\right) \\ &\cos\left(\alpha^T(t) - \alpha_v\right) + \cos\left(\beta^R(t)\right) \cos\left(\alpha_v - \alpha^R(t)\right) \Big] \\ &+ \sin(\beta_v(t)) \left[\sin\left(\beta^T(t)\right) + \sin\left(\beta^R(t)\right) \right] \Big\} \end{aligned} \tag{5}$$

where $f_{\max}(t) = v(t)/\lambda$ is the maximum Doppler frequency, with λ being the wavelength of the carrier signal and $v(t) = \sqrt{v_v^2 + v_h(t)^2}$ the speed of motion. The symbols $\beta^T(t)$, $\alpha^T(t)$, $\beta^R(t)$, $\alpha^R(t)$, and $\beta_v(t)$ stand for the elevation angle of departure, azimuth angle of departure, elevation angle of arrival, azimuth angle of arrival, and vertical angle of motion, respectively. According to [18], all these angles can be computed knowing the positions of the transmitter T_x and receiver R_x, the time variant position $(x(t), y(t), z(t))$, and speed $v(t)$ of the scatterer S^M.

Our assumptions on the speed profile, the person height, the head trajectory during the walk, the maximum speed during the fall, and the duration of the fall are all supported by measurements reported in the literature [14]–[16]. All these facts support the argument that our synthetic data is a reasonable approximation of real-word data. Moreover, to make our data generic, we simulated the activity of 30 participants with different heights, different walking speeds, and following different paths while performing their activities. This makes the data statistically uncorrelated and reflects the diversity generally observed in real-world data.

IV. Data Pre-Processing

A. Data Filtering

The developed channel simulator allows us to generate complex channel gain data pertaining to the activity of 30 different individuals. This data is fingerprinted by the activity performed by the user. In order to recognize the performed activity from the complex channel gain $\mu(t)$, we need first to pre-process the collected data. As it is obvious from (4), the complex channel gain $\mu(t)$ encompasses the contribution of both moving and fixed scatterers. Intuitively, it would be easier to classify the activity based on the complex channel gain component associated with the moving scatterer. Therefore, it is of interest to remove the multipath components pertaining to the fixed scatterers. Note that the fixed scatterers' contribution to the channel gain is an unknown constant term, which implies that this term is a zero-frequency component. Hence, it is possible to remove the contribution of all fixed scatterers by applying a high-pass filter to the complex channel gain $\mu(t)$. To this end, we utilize a Chebyshev filter of Type II [19] with a stopband attenuation of 40 dB and a stopband frequency of 0.05 Hz. The choice of a Type II Chebyshev filter is motivated by its sharpness and the fact that it has no ripples for frequencies larger than the passband frequency [19]. These characteristics allow extracting the contribution of the moving scatterers in the complex channel gain $\mu(t)$ with very minor distortions. The filtered complex channel gain $\hat{\mu}(t)$ is a good approximation of the contribution of the moving scatterer, i.e.,

$$\hat{\mu}(t) \quad = \quad \mu(t) * h(t) \approx c_m \exp\left[j\theta_m(t)\right], \qquad (6)$$

where $h(t)$ denotes the impulse response of the Chebyshev filter of Type II.

B. Instantaneous Doppler Frequency Estimation

In this section, we propose a method for estimating the instantaneous Doppler frequency of non-stationary signals. Our starting point is the filtered complex channel gain $\hat{\mu}(t)$ which can be regarded as a mono-component signal with time-variant frequency. Our proposed estimation method comprises the following steps:

1) Extract the phase $\hat{\theta}_m(t)$ of the signal $\hat{\mu}(t)$.
2) Determine an estimate $\hat{f}_m(t)$ of the instantaneous Doppler frequency as $\hat{f}_m(t) = \frac{d(\hat{\theta}_m(t))}{2\pi\, dt}$.
3) Apply a Gaussian smoothing filter to remove the ripples in the estimated instantaneous Doppler frequency $\hat{f}_m(t)$. The obtained instantaneous Doppler frequency after smoothing is denoted as $\tilde{f}_m(t)$.

Next, we numerically evaluate the accuracy of the proposed estimation method. We consider two data buffers associated with walking and slow fall. In Fig. 2, we illustrate the estimated and the exact instantaneous Doppler frequency $f_m(t)$ for a walking and slow fall scenarios. From this figure, the high accuracy of the proposed estimation method in determining the instantaneous Doppler frequency $f_m(t)$ is noticeable. For the slow fall scenario in Fig. 2, the participant walks for 1 s, and then he starts falling. The fall lasts for 2 s, i.e., from $t = 1$ s to $t = 3$ s. After the fall, the person remains on the ground without any movement, and consequently his instantaneous Doppler frequency $f_m(t)$ becomes zero.

V. Machine Learning Framework

Our aim is to recognize three different human activities based on the recorded complex channel gain.

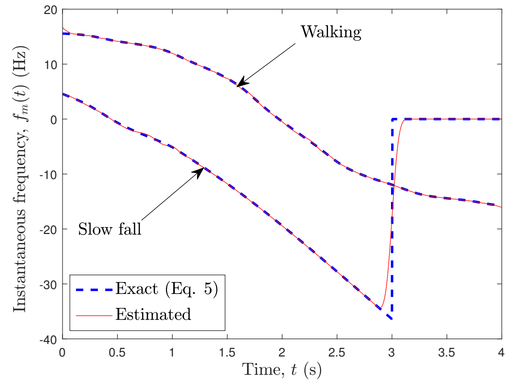

Fig. 2: Instantaneous Doppler frequency $f_m(t)$ for a walking scenario.

These activities are walking, slow fall, and fast fall. To achieve our goal, we use a supervised machine learning approach and train a set of classification algorithms to recognize human activity based on the recorded complex channel gain in an indoor environment. The various building blocks of the activity recognition scheme are illustrated in Fig. 3.

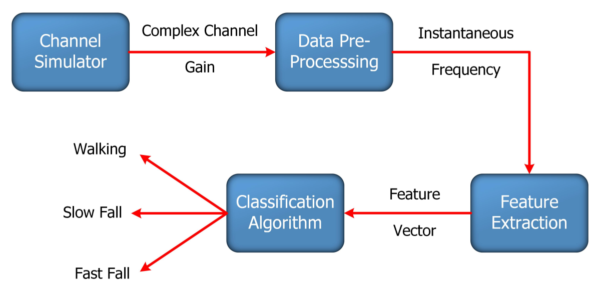

Fig. 3: Machine learning framework for activity recognition.

The first block is the channel simulator described in Sections II and III. The output of the channel simulator is the complex channel gain $\mu(t)$ that captures the impact of the fixed scatterers in the indoor environment as well as the impact of the moving person. The complex channel gain $\mu(t)$ is then fed to the data pre-processing block. This block first removes the impact of fixed scatterers using a high-pass filter as described in Section IV-A. Afterwards, we estimate the instantaneous Doppler frequency using the method proposed in Section IV-B. The instantaneous Doppler frequency becomes the input signal for the feature extraction block, which extracts four features from the instantaneous Doppler frequency, namely, the mean value, variance, root mean square (RMS), and maximum of the absolute value. These features are then stacked in a vector, called feature vector. The classification algorithm determines the type of the performed activity based on the feature vector. In the following, we discuss in more detail the feature extraction and the classification algorithm blocks.

A. Features Extraction

If the classification algorithm uses the raw data of the instantaneous Doppler frequency to determine the type of the performed activity, the obtained results would have very poor accuracy. To deal with this issue, we must extract a set of features that captures a quantitative description of each activity and allow us to distinguish different activities. We extract four features from the instantaneous Doppler frequency: (i) the mean, (ii) variance, (iii) RMS, and (iv) maximum of the absolute value. The RMS of the instantaneous Doppler frequency $\tilde{f}_m(t)$ can be expressed as

$$\tilde{f}_m^{rms} = \sqrt{\frac{1}{T}\int_0^T \left[\tilde{f}_m(t)\right]^2 dt} \tag{7}$$

where T is the length of the buffer which is equal to 4 s.

Fig. 4 depicts the histogram of the maximum value of $|\tilde{f}_m(t)|$ for the activities walking and fast fall. From this figure, one can see that the maximum value of $|\tilde{f}_m(t)|$ is between 7 and 20 Hz for the activity walking, while for fast falls the range of the maximum value of $|\tilde{f}_m(t)|$ is between 10 and 55.5 Hz. In fact, for fast falls, the velocity reaches larger values compared to walking scenarios, which results in much larger values of $|\tilde{f}_m(t)|$.

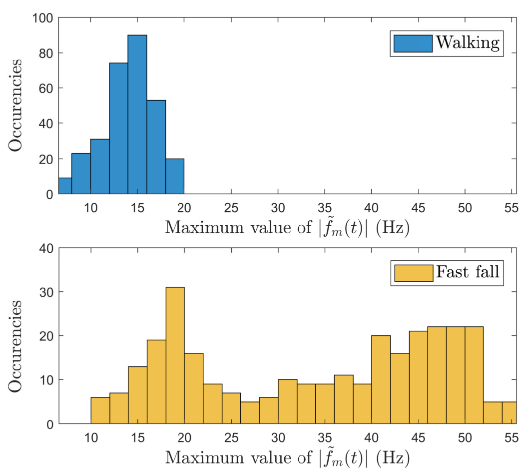

Fig. 4: Histogram of the maximum value of $|\tilde{f}_m(t)|$ for the activities walking and fast fall.

Fig. 5 illustrates the histogram of the variance of the instantaneous Doppler frequency $\tilde{f}_m(t)$ for walking and fast falls. This figure shows that the variance of $\tilde{f}_m(t)$ is mostly below 50 Hz^2 for walking, whereas, for fast falls the variance of $\tilde{f}_m(t)$ is mostly ranging from 10 to 200 Hz^2. This is due to the fact that the instantaneous Doppler frequency $\tilde{f}_m(t)$ has a larger dynamic range for fast falls compared to walking.

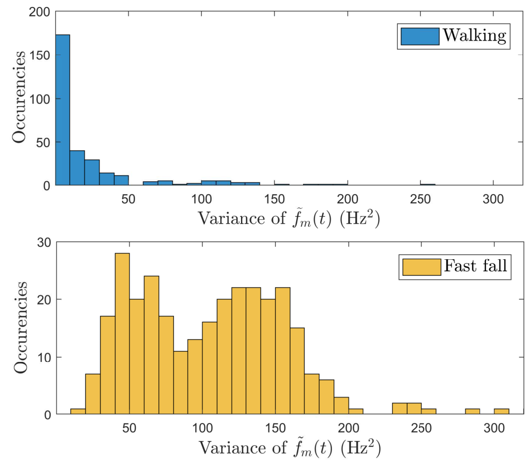

Fig. 5: Histogram of the variance of the instantaneous Doppler frequency $\tilde{f}_m(t)$ for the activities walking and fast fall.

B. Classification Algorithm

Classification algorithms follow a supervised learning approach to recognize different types of activities. The supervised learning approach consists of two phases: the training phase and test phase. First, the data is divided into buffers which are labeled with an activity identity (ID). We have three activity IDs: 1, 2, and 3 corresponding to walking, slow fall, and fast fall, respectively. Each data buffer has a length of 4 s and contains the recording of the complex channel gain, while a person is performing one of the three activities. The data buffer is then preprocessed, its features are extracted, and stored in a feature vector.

The data is divided into training and test data representing 70% and 30% of the total data, respectively. During the training phase, the classification algorithm is exposed to the labeled training data. This means that, for each data buffer in the training data, we provide the corresponding feature vector together with the activity ID. In this way, the classification algorithm can tune its internal parameters such that its recognition accuracy is maximized.

After the training phase, the trained classifier is exposed to the test data. In the test phase, for each buffer of the test data, the classifier is provided with the corresponding feature vector without the activity ID. The trained classifier uses the feature vector to determine the probability that the data buffer pertains to one of the three possible activities. If the activity class $i\,(i = 1, 2, 3)$ has the highest probability, the classifier decides that the performed activity has the ID i. The correctness of the classifier decision can be determined using the data buffer label. For each buffer in the test data, the classifier predicts the performed activity.

At the end of the test phase, we can assess the performance of the trained classifier and evaluate the accuracy and precision of its predictions. In this paper, we evaluated the performance of three classification algorithms, namely, decision tree, ANN, and cubic SVM. Principles and background information about these classification algorithms can be found in [20].

VI. Experimental Results

The performance of the proposed activity recognition framework is evaluated in this section. We use a supervised learning approach in which the classification algorithm is trained using 70% of the data. Once the training phase is complete, the trained classifier is tested using the remaining 30% of the data. We assess the performance of three different classification algorithms, namely, decision tree, ANN, and cubic SVM algorithms.

The confusion matrix of the decision tree algorithm is provided in Fig. 6. The labels 1, 2, and 3 at the bottom of the confusion matrix correspond to the activities walking, slow fall, and fast fall. The overall accuracy of the decision tree algorithm is 73% as shown in the bottom diagonal cell of the confusion matrix. The remaining diagonal cells indicate the number and percentage of correct classifications by the trained decision tree algorithm. The classifier correctly predicts the activities walking, slow fall, and fast fall in 68, 82, and 47 cases, respectively. The first column of the confusion matrix in Fig. 6 shows that there are a total of 90 walking buffers, of which 68 buffers are correctly classified, while 22 buffers are misclassified as slow fall. This implies that the accuracy of the algorithm in recognizing the activity walking is 75.6%. By examining the bottom cells of the second and third columns, we can see that the accuracy of the classifier for the activities slow fall and fast fall equals 91.1% and 52.2%, respectively.

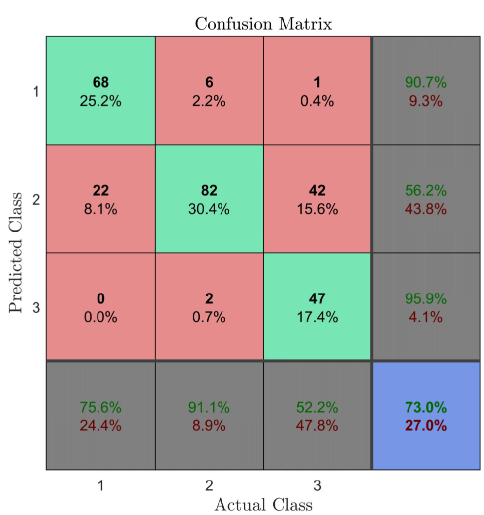

Fig. 6: Confusion matrix of the decision tree algorithm.

The rows of the confusion matrix in Fig. 6 indicate the precision of the classifier for the three activities. For instance, the second row shows the buffers which are classified as slow fall. In total there are 146 buffers classified as slow fall. Out of these, 82 buffers are real slow falls, while 22 and 42 buffers correspond to the activities walking and fast fall, respectively. Thus, the precision of the classifier for slow falls is 56.2%. The last cell in the first row and the third row indicate a precision of 90.7% and 95.9% for walking and fast fall, respectively.

Note that the precision and the accuracy of the classification have different meanings. The classification precision focuses on the predicted activity. For a given activity, the precision quantifies the percentage of correct classifications out of the buffers predicted to belong to that certain activity. On the contrary, the classification accuracy focuses on the actual activity and indicates the percentage of successful classifications out of the actual buffers belonging to a given class.

The confusion matrices of the ANN and cubic SVM algorithms are illustrated in Figs. 7 and 8, respectively. From these figures, we observe that the overall accuracy of the ANN and cubic SVM is 84.1% and 92.6%, respectively, which represents an enhancement of 11.1% and 19.6% compared to the decision tree algorithm. For the ANN algorithm, the classification accuracy for the activities walking, slow fall, and fast fall is equal to 91.1%, 84.5%, and 77%, respectively. The classification precision of the ANN for the activities walking, slow fall, and fast fall is equal to 85.9%, 74.7%, and 92.8%, respectively.

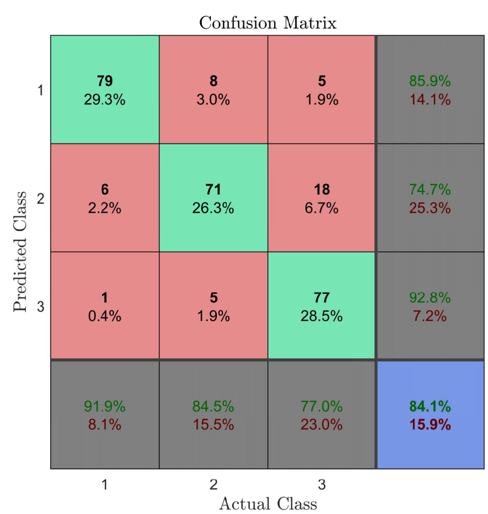

Fig. 7: Confusion matrix of the ANN algorithm.

The cubic SVM algorithm outperforms the decision tree and the ANN algorithms in terms of overall accuracy, precision, and accuracy per activity. Compared with the decision tree algorithm, the cubic SVM enhances the classification accuracy of the activities walking, slow fall, and fast fall by 18.8%, 6.7%, and 33.4%, respectively. Moreover, the cubic SVM improves the classification precision by 8.1%, 28.4%, and 0.4% for the activities walking, slow fall, and fast fall, respectively, compared to the decision tree algorithm.

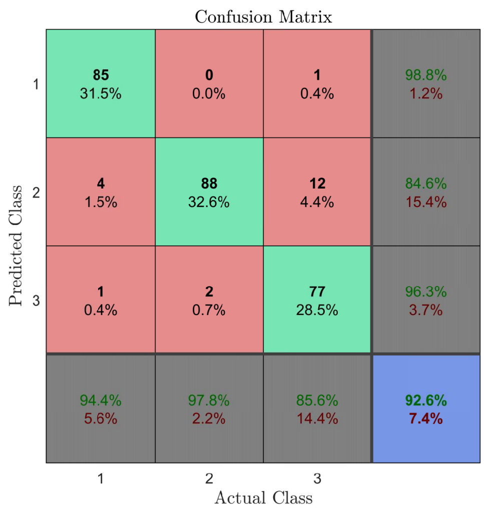

Fig. 8: Confusion matrix of the cubic SVM algorithm.

VII. Conclusion

This paper has developed an activity simulator that generates the complex channel gain of indoor channels in the presence of one person performing three different activities, namely, slow fall, fast fall, and walking. Using this activity simulator, we created complex channel gain data associated with 30 participants having different heights, speed profiles, and trajectories. We have proposed a novel method for extracting the instantaneous Doppler frequency with high accuracy from the complex channel gain. Moreover, we have built a machine learning framework for activity recognition based on the instantaneous Doppler frequency. Using the generated complex channel gain, we have tested the performance of the decision tree, ANN, and cubic SVM classification algorithms in recognizing human activities. First, these three algorithms have been optimized using the training data, then their performances have been evaluated using the test data. Our investigation reveals that the cubic SVM algorithm outperforms the decision tree and ANN algorithms in terms of overall accuracy. The decision tree, ANN, and cubic SVM achieve an overall activity recognition accuracy of 73%, 84.1%, and 92.6%, respectively.

References

[1] The World Bank. (2017, Jun.) Population ages 65 and above, total. [Online]. Available: https://data.worldbank.org/indicator/SP.POP.65UP.TO?end=2017&start=1960

[2] The World Health Organization. (2018, Jun.) World report on ageing and health. [Online]. Available: http://apps.who.int/iris/bitstream/handle/10665/186463/9789240694811_eng.pdf

[3] C. Florence *et al.*, "Medical costs of fatal and nonfatal falls in older adults," *Journal of the American Geriatrics Society*, Mar. 2018, DOI: 10.1111/jgs.15304.

[4] G. Bergen, M. Stevens, and E. Burns. (2018, Jun.) Falls and fall injuries among adults aged $\geq$ 65 years – United States, 2014. DOI: 10.15585/mmwr.mm6537a2.

[5] R. Igual, C. Medrano, and I. Plaza, "Challenges, issues and trends in fall detection systems," *BioMedical Engineering OnLine*, vol. 12, no. 1, pp. 1–24, Jul. 2013.

[6] K. Sehairi, F. Chouireb, and J. Meunier, "Comparative study of motion detection methods for video surveillance systems," *Journal of Electronic Imaging*, vol. 26, no. 2, pp. 26–29, Apr. 2017.

[7] A. Sucerquia, J. D. López, and J. F. Vargas-Bonilla, "SisFall: A fall and movement dataset," *Sensors*, vol. 17, no. 1, pp. 1–14, Jan. 2017, DOI: 10.3390/s17010198.

[8] A. Chelli and M. Pätzold, "Recognition of falls and daily living activities using machine learning," in *29th IEEE Int. Symp. on Pers., Indoor, and Mobile Radio Commun. (PIMRC'18)*, Bologna, Italy, Sep. 2018.

[9] Y. Wang, K. Wu, and L. M. Ni, "WiFall: device-free fall Detection by wireless networks," *IEEE Transactions on Mobile Computing*, vol. 16, no. 2, pp. 581–594, Feb. 2017.

[10] F. Adib, Z. Kabelac, D. Katabi, and R. C. Miller, "3D tracking via body radio reflections," in *11th USENIX Conf. Netw. Syst. Des. Implementation*, vol. 14, Seattle, WA, USA, Apr. 2014, pp. 317–329.

[11] H. Abdelnasser, M. Youssef, and K. A. Harras, "WiGest: A ubiquitous WiFi-based gesture recognition system," in *IEEE Conference on Computer Communications (INFOCOM 2015)*, Hong Kong, China, Apr. 2015, pp. 1472–1480.

[12] F. Adib and D. Katabi, "See through walls with WiFi!" in *ACM SIGCOMM Conf. SIGCOMM, 2013*, Hong Kong, China, Aug. 2013, pp. 75–86.

[13] T. Oberg, A. Karsznia, and K. Oberg, "Basic gait parameters: reference data for normal subjects, 10-79 years of age," *Journal of Rehabilitation Research and Development*, vol. 30, no. 2, pp. 210–223, 1993.

[14] A. K. Bourke, M. Torrent, X. Parra, A. Català, and J. Nelson, "Fall algorithm development using kinematic parameters measured from simulated falls performed in a quasi-realistic environment using accelerometry," in *2011 Ann. Int. Conf. of the IEEE Engineering in Medicine and Biology Society*, Boston, MA, USA, Aug. 2011, pp. 4449–4452.

[15] G. Wu, "Distinguishing fall activities from normal activities by velocity characteristics," *Journal of Biomechanics*, vol. 33, no. 11, pp. 1497 – 1500, 2000, DOI: 10.1016/S0021-9290(00)00117-2.

[16] S.-U. Jung and M.-S. Nixon, "Estimation of 3D head region using gait motion for surveillance video," in *4th International Conference on Imaging for Crime Detection and Prevention 2011, ICDP 2011*. London, UK, Nov. 2011, pp. 1–6, DOI: 10.1049/ic.2011.0105.

[17] A. Abdelgawwad and M. Pätzold, "On the influence of walking people on the Doppler spectral characteristics of indoor channels," in *28th IEEE Int. Symp. on Pers., Indoor, and Mobile Radio Commun. workshops (PIMRC'17)*, Montreal, QC, Canada, Oct. 2017.

[18] ——, "A framework for activity monitoring and fall detection based on the characteristics of indoor channels," in *87th IEEE Vehicular Technology Conference (VTC Spring 2018)*, Porto, Portugal, Jun. 2018, pp. 1–7.

[19] A. B. Williams and F. J. Taylor, *Electronic Filter Design Handbook*, 4th ed. New York, USA: McGraw-Hill, 2006.

[20] C. M. Bishop, *Pattern Recognition and Machine Learning*, 1st ed. Cambridge, UK: Springer, 2006.